Eur. Phys. J. B (2017) 90: 30
DOI: 10.1140/epjb/e2017-70482-4

THE EUROPEAN PHYSICAL JOURNAL B

Regular Article

Extreme-volatility dynamics in crude oil markets

Xiong-Fei Jiang[1,2,3,a], Bo Zheng[3,4], Tian Qiu[5], and Fei Ren[6]

[1] School of Information Engineering, Ningbo Dahongying University, Ningbo 315175, P.R. China
[2] Research Center for Finance Computing, Ningbo Dahongying University, Ningbo 315175, P.R. China
[3] Department of Physics, Zhejiang University, Hangzhou 310027, P.R. China
[4] Collaborative Innovation Center of Advanced Microstructures, Nanjing 210093, P.R. China
[5] School of Information Engineering, Nanchang Hangkong University, Nanchang 330063, P.R. China
[6] School of Business, East China University of Science and Technology, Shanghai 200237, P.R. China

Received 15 August 2016 / Received in final form 21 November 2016
Published online 13 February 2017 –

Abstract. Based on concepts and methods from statistical physics, we investigate extreme-volatility dynamics in the crude oil markets, using the high-frequency data from 2006 to 2010 and the daily data from 1986 to 2016. The dynamic relaxation of extreme volatilities is described by a power law, whose exponents usually depend on the magnitude of extreme volatilities. In particular, the relaxation before and after extreme volatilities is time-reversal symmetric at the high-frequency time scale, but time-reversal asymmetric at the daily time scale. This time-reversal asymmetry is mainly induced by exogenous events. However, the dynamic relaxation after exogenous events exhibits the same characteristics as that after endogenous events. An interacting herding model both with and without exogenous driving forces could qualitatively describe the extreme-volatility dynamics.

1 Introduction

Crude oil is one of the most important commodities in the world. Crude oil prices significantly affect the global economy. Low crude oil prices often lead to an economic depression in oil exporting countries, while high oil prices may increase inflation. Therefore, a better understanding of the price movements becomes a fundamental issue in the crude oil markets. Various methods from diverse disciplines have been proposed to forecast the price movements in the crude oil markets. The GARCH-class models are the common methods for forecasting the volatility persistence [1,2]. Machine-learning algorithms, such as the neural network [3] and the support vector machine [4,5], have played an important role in forecasting crude oil prices. Additionally, various other methods, including predictive regressions with economic restrictions [6] and the dynamic model averaging approach [7], have been also introduced to predict crude oil prices.

An important factor causing the failure of predictions is characterized by unpredictable extreme volatilities, which may drive the crude oil markets to a non-stationary state [8]. For improving the predicting accuracy, therefore, it is crucial to understand the dynamic behavior of extreme volatilities. Extreme volatilities in the crude oil markets have received widespread attention in recent years. The recurrence intervals of extreme volatilities of the energy futures have been investigated [9], and it has been demonstrated that the 2006–2008 oil bubble was amplified by the speculative behavior [10]. With the empirical mode decomposition, it is observed that the extreme events show a medium time impact on the crude oil markets, while the irregular events only have a short-term effect [11]. Some works also consider the impact of extreme volatilities on the forecasting models [11,12].

On the other hand, there has been great success in recent research of the stock markets using the methods of statistical physics [13–18]. Therefore, it is natural to extend these methods to the field of the crude oil markets. For example, the return-volatility correlation has been investigated in energy futures recently [19]. In particular, extreme-volatility dynamics have been widely studied in the stocks markets. After extreme crashes, the rate of volatilities larger than a specific threshold decreases by a power law [20], which is analogous to the Omori law characterizing the aftershocks of a huge earthquake [21]. The Omori law is also observed in the daily data of financial indices for several emerging stock markets after the two largest crashes [22]. The dynamic behavior of the volatility has been determined around extreme events [23]. The volatility dynamics driven by interest-rate change have been investigated in the US stock market [24].

However, non-stationary dynamics are still an open question in complex systems. For example, the correlation function nonlocal in time is constructed to investigate the volatility-return correlation in financial dynamics [25]. In particular, we have recently developed a theoretical

[a] e-mail: xfjiang@nbdhyu.edu.cn

framework based on concepts and methods in statistical physics, for analyzing the non-stationary dynamics of extreme events in complex systems [26]. In this paper we introduce this framework to systematically explore extreme-volatility dynamics in the crude oil markets, based on high-frequency data and daily data. We investigate the dynamic relaxation both before and after the extreme volatilities, and observe the time-reversal symmetry or asymmetry at different time scales. We examine the dynamic behavior of different categories of extreme volatilities, and search for the origin of the time-reversal asymmetry at the daily time scale. Finally, we introduce an interacting EZ model to simulate the extreme-volatility dynamics.

2 Data and methodology

We have collected the daily data of crude oil prices for the West Texas Intermediate (WTI) Spot and Future, from Jan. 2, 1986 to Oct. 11, 2016, with 7765 and 7722 trading days respectively. The high-frequency data are the minute-to-minute prices of the fuel oil future in the Shanghai Futures Exchange, from Jan. 16, 2006 to Jun. 25, 2010, with 221 427 data points. The high-frequency data are recorded every minute, and a working day is exactly 215 min in the Shanghai Futures Exchange.

We define the logarithmic return over a time interval of one day and one minute for the daily and high-frequency data respectively,

$$R\left(t'\right) \equiv \ln\, P\left(t'+1\right) - \ln\, P\left(t'\right), \tag{1}$$

where $P\left(t'\right)$ represents the oil price at time t'. For simplicity, the volatility is then defined as the absolute value of returns, $|R\left(t'\right)|$. To investigate the dynamic relaxation before and after the extreme volatilities, let us introduce the anti-remanent and remanent volatilities $v_{-}(t)$ and $v_{+}(t)$,

$$v_{\pm}(t) = \left[\langle |R\left(t' \pm t\right)| \rangle_c - \sigma\right]/Z, \tag{2}$$

where $Z = \langle |R\left(t'\right)| \rangle_c - \sigma$, σ is the average volatility, and $\langle \cdots \rangle_c$ represents the average over those times t' which fulfill the extreme volatility condition. In this paper, we determine the extreme volatilities with the condition $|R\left(t'\right)| > \zeta$, where the given threshold ζ is well larger than σ. It represents the crashes and rallies in the crude oil markets, if ζ is sufficiently large. $v_{-}(t)$ describes how the dynamic system approaches an extreme volatility from the stationary state, while $v_{+}(t)$ illustrates how it relaxes from an extreme volatility.

Extreme volatilities in financial markets are usually followed by a series of aftershocks, showing long-range correlations [20,22,26]. Therefore, it is reasonable to assume that both $v_{\pm}(t)$ follow a power law,

$$v_{\pm}(t) \sim \left(t + \tau_{\pm}\right)^{-p_{\pm}}, \tag{3}$$

where $p_{\pm}$ are the exponents and $\tau_{\pm}$ are positive constants. The constants $\tau_{\pm}$ are rather small for most cases in this paper. To reduce the fluctuations, we integrate both sides of equation (3) from 0 to t. The cumulative function of $v_{\pm}(t)$ is then written as

$$V_{\pm}(t) \sim \left[\left(t + \tau_{\pm}\right)^{1-p_{\pm}} - \tau_{\pm}^{1-p_{\pm}}\right], \tag{4}$$

where $p_{\pm} \neq 1$. The power-law behavior of $V_{\pm}(t)$ actually represents the long-range temporal correlation of volatilities. Such a power-law behavior has been well studied in dynamic critical phenomena, even in cases far from equilibrium [27,28].

Table 1. The exponents $p_{\pm}$ with $\tau_{\pm} = 0$ for the high-frequency data of the fuel oil future, fitted with equation (4).

ζ	2σ	4σ	6σ	8σ
$p-$	0.14(1)	0.17(1)	0.20(1)	0.21(1)
$p+$	0.13(1)	0.15(1)	0.18(1)	0.20(1)

3 Results

We first analyze the high-frequency data of the fuel oil future in the Shanghai Futures Exchange. Here $|R(t)|$ is calculated on the minute time scale. We set the threshold $\zeta = 2\sigma$, 4σ, 6σ and 8σ to determine extreme volatilities. For the high-frequency data, an extreme volatility might drive the dynamic system to a microscopic non-stationary state, but it may not represent an exact macroscopic crash or rally. In Figure 1a, $V_{\pm}(t)$ of the high-frequency data are showed on a log-log scale.

Due to the intra-day pattern [29–31], both $V_{\pm}(t)$ periodically fluctuate at $t = 215$ min, i.e., a working day in the Shanghai Futures Exchange. This kind of intra-day pattern originates from price jumps between the closing price and the opening price of the next day. To exclude the intra-day pattern, we define the intra-day pattern factor $D(t'_{day})$ as

$$D\left(t'_{day}\right) = \frac{1}{N}\sum |R_j\left(t'_{day}\right)|, \tag{5}$$

where j runs over all the trading days N, and t'_{day} is the time in a trading day. Then we normalized the volatility at time $t' = t'_{day}$ as

$$r\left(t'_{day}\right) = |R\left(t'_{day}\right)|/D\left(t'_{day}\right). \tag{6}$$

Then $V_{\pm}(t)$ are recalculated with $r(t'_{day})$. As displayed in Figure 1b, both $V_{\pm}(t)$ for $r(t'_{day})$ show an almost perfect power-law behavior.

Fitting the curves of $V_{\pm}(t)$ to equation (4), we obtain the exponents $p_{\pm}$ summarized in Table 1. Both $p_{\pm}$ increase with the threshold ζ. In particular, p_{+} and p_{-} of every ζ are equal within statistical errors. Namely, the dynamic relaxation is symmetric before and after the extreme volatilities at the microscopic time scale, i.e., the minute time scale.

For better understanding the extreme-volatility dynamics of crude oil prices, we have calculated $V_{\pm}(t)$

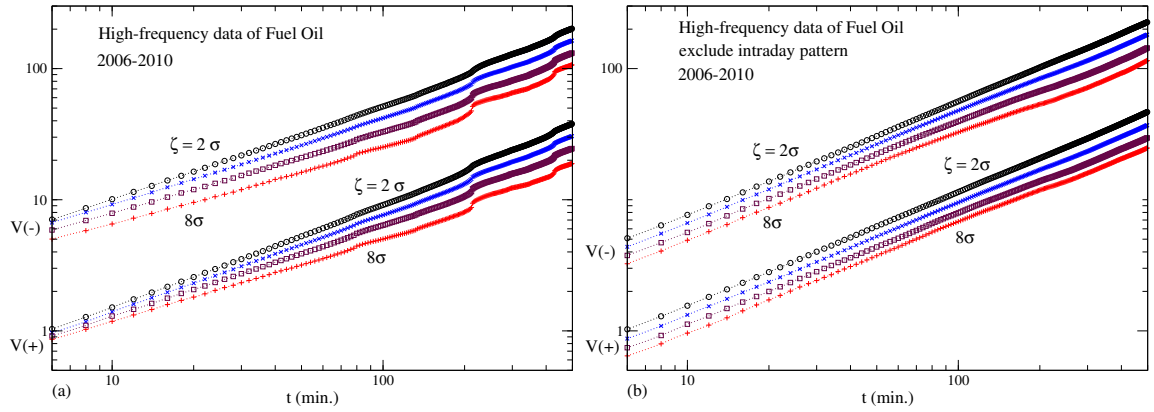

Fig. 1. (a) $V_{\pm}(t)$ for the high-frequency data of the fuel oil future in the Shanghai Futures Exchange. From above, the threshold is $\zeta = 2\sigma$, 4σ, 6σ and 8σ respectively. (b) The same as (a), but the intra-day pattern has been removed.

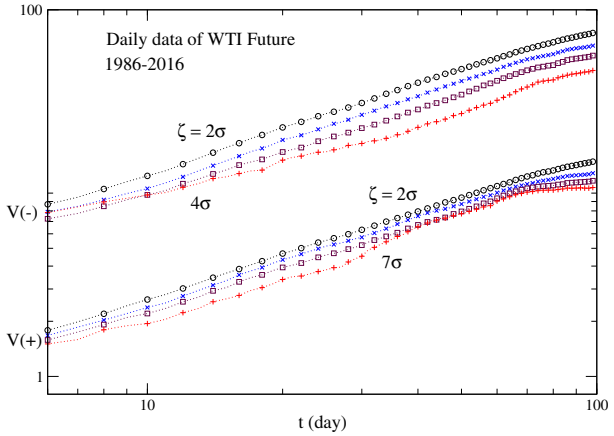

Fig. 2. $V_{\pm}(t)$ for the daily data of the WTI Future. From above, the threshold is $\zeta = 2\sigma$, 4σ, 5σ, and 7σ respectively. For clarity, some curves have been shifted downwards or upwards.

with the daily data of the WTI Spot and Future. The extreme volatilities for the daily data are determined with $\zeta = 2\sigma$, 4σ, 5σ and 7σ. As displayed in Figure 2, $V_{\pm}(t)$ for the WTI Future could also be characterized by equation (4). Compared with those of the high-frequency data, the curves of the daily data are somewhat fluctuating. We obtain the exponents $p_{\pm}$ of the daily data with $\tau_{\pm} = 0$, summarized in Table 2. p_{-} of the daily data is ζ-dependence obvious. However, ζ-dependence for p_{+} is weaker, leading to $p_{-} \neq p_{+}$. In other words, the time-reversal symmetry before and after the extreme volatilities is violated at the daily time scale. Similar results are obtained for the WTI Spot.

What is the underlying mechanism for the violation of the time-reversal symmetry before and after extreme volatilities at the daily time scale? Addressing this question is a natural way to investigate the dynamic relaxation of different categories of extreme volatilities, since the extreme volatilities may originate differently. We classify extreme volatilities $|R(t')|$ with $R(t') > 0$ and $R(t') < 0$, which are the "rallies" and "crashes" respectively. Then $V_{\pm}(t)$ are calculated for the rallies and crashes separately,

Table 2. The exponents $p_{\pm}$ with $\tau_{\pm} = 0$ for the daily data, fitted with equation (4). The first sector is $p_{\pm}$ for the WTI Future, and the second sector is $p_{\pm}$ for the WTI Spot.

ζ	2σ	4σ	5σ	7σ
	Future			
$p-$	0.17(1)	0.22(1)	0.27(1)	0.35(3)
$p+$	0.16(1)	0.20(2)	0.23(2)	0.23(4)
	Spot			
$p-$	0.20(1)	0.24(2)	0.26(2)	0.33(3)
$p+$	0.19(1)	0.21(2)	0.20(2)	0.23(3)

and fitted to equation (4). At the high-frequency time scale, the exponents $p_{\pm}$ remain the same both for the crashes and rallies, as shown in Figure 3. At the daily time scale, $p_{\pm}$ of the crashes and rallies are also only marginally different both for the WTI Spot and WTI Future. In other words, crude oil markets do not distinguish between the crashes and rallies for the extreme-volatility dynamics.

Extreme volatilities at the daily time scale could also be classified into endogenous events and exogenous events [26,32,33]. Generally, an exogenous event is related to the market's response to external forces, such as policy changes or wars. An endogenous event is driven by the internal dynamics of the system. In this paper, we mainly classify these events by the reports from the International Energy Agency and the Energy Information Administration. Looking carefully at the history of the crude oil markets, we confirm 11 exogenous events among 36 extreme volatilities selected by the threshold $\zeta \geq 6\sigma$ for the WTI Future, and 12 exogenous events among 33 extreme volatilities for the WTI Spot. It is not meaningful to identify the external forces for the extreme volatilities corresponding to the lower thresholds such as $\zeta = 2\sigma$ and 4σ. In Figure 4 and 5, $V_{\pm}(t)$ of $\zeta = 5\sigma$ and 7σ are plotted for the endogenous and exogenous events separately, and the exponents $p_{\pm}$ are summarized in Table 3.

It is observed that the relaxation dynamics before and after the extreme volatility is symmetric for the endogenous events, i.e., $p_{-} \approx p_{+}$, while asymmetric for the exogenous events, i.e., $p_{-} > p_{+}$. In other words,

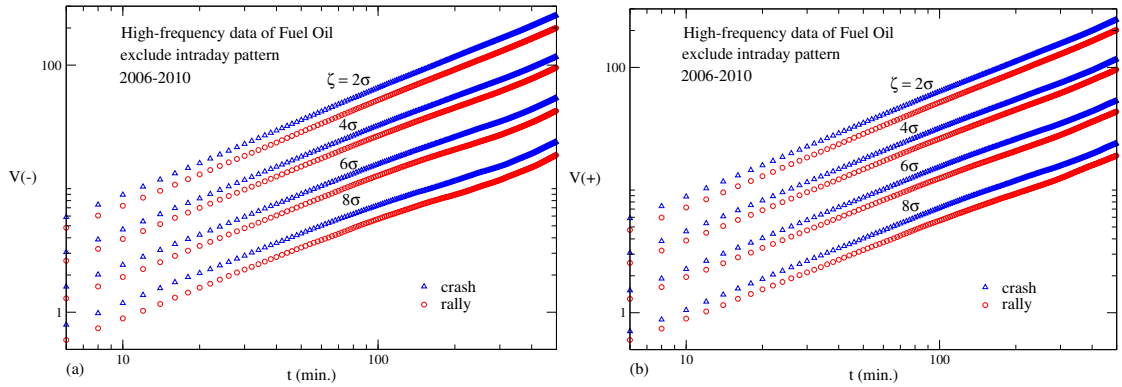

Fig. 3. $V_{\pm}(t)$ for the crashes and rallies of the high-frequency data are displayed for the fuel oil future in the Shanghai Futures Exchange. The intra-day pattern is removed. From above, the threshold is $\zeta = 2\sigma$, 4σ, 6σ and 8σ respectively.

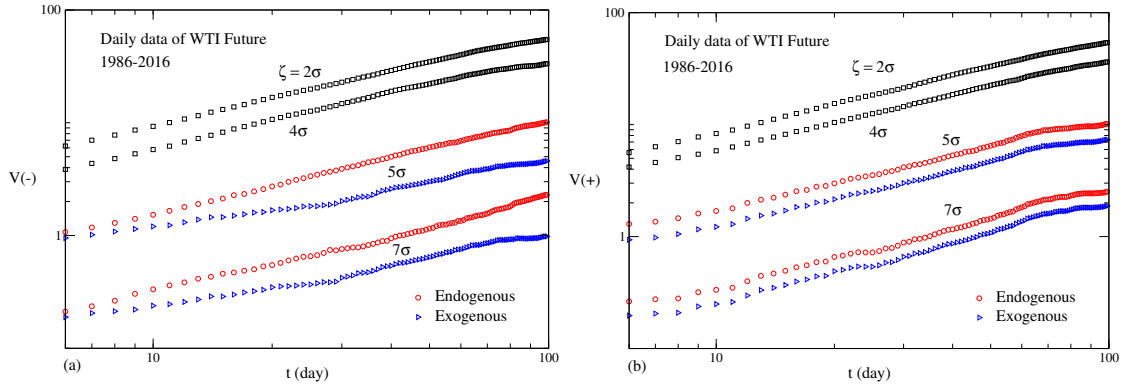

Fig. 4. For the daily data of the WTI Future, and with the thresholds of $\zeta = 5\sigma$ and 7σ, $V_{\pm}(t)$ are displayed for endogenous and exogenous events separately.

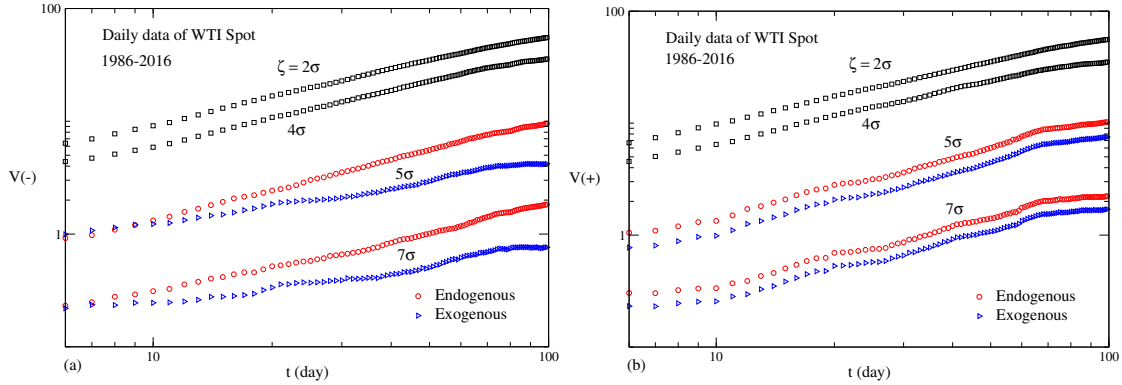

Fig. 5. For the daily data of the WTI Spot, and with the thresholds of $\zeta = 5\sigma$ and 7σ, $V_{\pm}(t)$ are displayed for endogenous and exogenous events separately.

the time-reversal asymmetry of the dynamic relaxation before and after the extreme volatility at the daily time scale is induced by the exogenous events, not by the endogenous events. This violation of the time-reversal symmetry at the macroscopic time scale is also observed in the traditional physics system. For instance, the microscopic equations of motion reversible in time may result in irreversible macroscopic dynamic processes [28].

Considering that $V_{-}(t)$ describes how a crude oil market approaches an extreme volatility, it is reasonable that p_{-} of the exogenous events is larger than p_{-} of the endogenous events, since an exogenous event should arise more suddenly than an endogenous event. On the other hand, keeping in mind that p_{+} of the exogenous and p_{+} of endogenous events are almost equal, it seems that once the extreme events occur, the dynamic relaxation of the crude oil markets does not distinguish between exogenous and endogenous events. Such a phenomenon is similar to the behavior of the mature stock market, e.g., the German market, while different from the behavior of the emerging stock market, e.g., the Chinese market. This may imply that the crude oil market is a mature asset market.

Table 3. The exponents $p_\pm$ with $\tau_\pm = 0$ for the endogenous (EN.) and exogenous (EX.) events, fitted with equation (4) for the daily data of the WTI Future and WTI Spot.

ζ	2σ	4σ	5σ	7σ	
	Future				
$p-$	0.17(1)	0.22(1)	0.21(2)	0.23(3)	En.
$p-$			0.35(3)	0.45(4)	Ex.
$p+$	0.16(1)	0.20(2)	0.23(2)	0.22(2)	En.
$p+$			0.24(2)	0.23(3)	Ex.
	Spot				
$p-$	0.20(1)	0.24(2)	0.21(3)	0.24(4)	En.
$p-$			0.38(3)	0.49(4)	Ex.
$p+$	0.19(1)	0.21(2)	0.20(2)	0.23(3)	En.
$p+$			0.21(3)	0.22(4)	Ex.

Table 4. The exogenous events corresponding to $\zeta \geq 6\sigma$ for the WTI Spot. IEA: International Energy Agency. OPEC: Organization of the Petroleum Exporting Countries.

Date	Event		ζ
1990.8.6	Rally	Iraq-Kuwait War	8σ
1990.10.22	Crash	IEA release reserved crude oil	8σ
1991.1.17	Crash	The Gulf War	8σ
1991.1.28	Crash	The Gulf War	7σ
1998.4.23	Crash	Asia Financial Crisis	7σ
1998.12.17	Crash	Asia Financial Crisis	7σ
2003.3.26	Crash	Iraq War	8σ
2008.9.23	Crash	Subprime mortgage crisis	7σ
2008.10.10	Crash	Subprime mortgage crisis	6σ
2008.12.1	Crash	Subprime mortgage crisis	6σ
2008.12.26	Rally	OPEC cut oil production	7σ
2008.12.31	Rally	OPEC cut oil production	7σ

4 Discussion

Different sorts of external forces may induce different extreme-volatility dynamic processes, and different markets may respond differently to the external forces. For example, all the exogenous events in the Shanghai stock market are generated by market-policy changes, while those in the German stock market correspond to political and economic accidents. However, the exogenous events in the crude oil markets are a mixture of market-policy changes and political or economic accidents, as shown in Table 4.

For the WTI Future, we identify 11 exogenous events among 36 extreme volatilities with $\zeta \geq 6\sigma$. For these exogenous events, 3 events drive the WTI Future to rallies, and 8 events led to crashes. The identified exogenous events are listed in Table 4. For endogenous events, 13 events caused crashes and 12 events resulted in rallies. Similar results are obtained for the WTI Spot. The only difference between the two markets is that the subprime mortgage crisis led to two crashes for the WTI Future, while resulting in three crashes for the WTI Spot. Unlike in the stock markets, the response to external forces is more complicated in the crude oil markets. For example, exogenous events usually create crashes, while endogenous events generate rallies in the German stock market [26].

The dynamic relaxation of the exogenous events is time-reversal asymmetric, i.e., $p_- \neq p_+$, while that of the endogenous events is approximately time-reversal symmetric, i.e., $p_- \approx p_+$. To quantitatively measure the difference between the endogenous events and exogenous events, we introduce an asymmetric factor f to characterize extreme volatilities,

$$f = \frac{\Sigma_+ - \Sigma_-}{\Sigma_+ + \Sigma_-}, \tag{7}$$

where $\Sigma_\pm$ are the areas bounded by the curves of $V_\pm(t)$ and the coordinate axes. Careful analysis shows that $f > 0.16$ and $f < 0.16$ reasonably classify exogenous and endogenous events respectively for both the WTI Spot and Future. These calculations confirm that the time-reversal asymmetry at the daily time scale is mainly induced by exogenous events.

5 Simulation

Although there have been many activities devoted to the macroscopic description of financial crashes [34–36], it remains a great challenge to simulate the dynamic relaxation of extreme volatilities at the microscopic level. A Gaussian process or a usual minority game fails to explain the extreme-volatility dynamics. In this paper, we present an interacting herding model first introduced in [37], which may qualitatively reproduce the dynamic behavior of the extreme volatilities. The model consists of N agents, which form clusters during dynamic evolution. Initially, each agent is a cluster. The dynamics evolve in the following way.

(1) At time step t', an agent i is selected randomly.
(2) With probability a, the agent i becomes active and decides buying or selling, and all agents in its cluster follow. After that, this cluster is broken into a state where each agent is a separate cluster. The size of this cluster is then recorded as $s(t')$.
(3) With probability $1 - a$, the agent i remains inactive. Another agent j is randomly selected. If agents i and j are in different clusters, combine the two clusters into a bigger one.

The parameter a apparently controls the dynamic evolution. In fact, $1/a$ is the rate of transmission of information [37]. Practically, one assumes that $s(t')$ is proportional to the volatility at time t'. If a is a constant, the model does not produce the long-range auto-correlation of volatilities. To mimic the real markets, a should not be a constant. For example, a may interact with the volatility in a form like [38,39],

$$a(t') = b + \frac{c}{s(t'-1)}. \tag{8}$$

Here b and c are positive constants. Such an interaction may generate a long-range auto-correlation of volatilities. We have performed the simulations with $N = 40\,000$ and $b = 0.00025$. The critical value of c is estimated to be 0.6. $V_\pm(t)$ is then calculated, and displayed in Figure 6a.

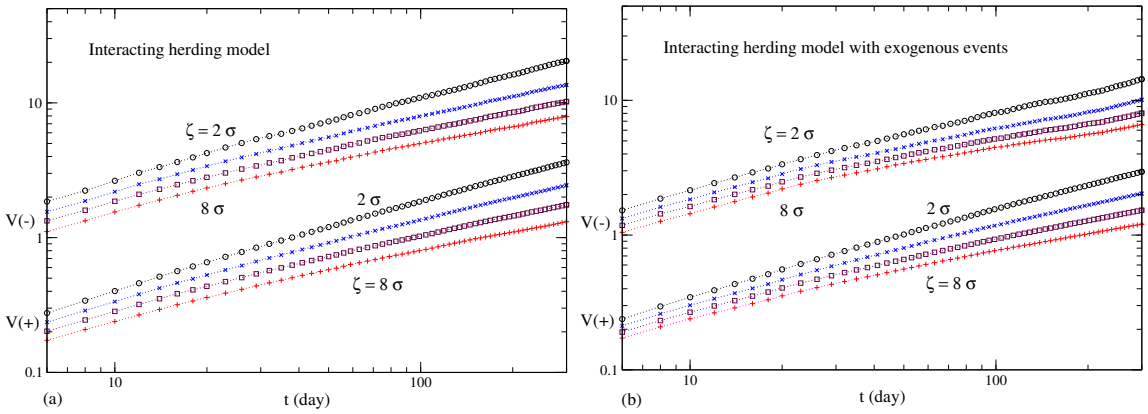

Fig. 6. $V_{\pm}(t)$ for the interacting herding model and its variant with exogenous driving forces. From above, the threshold is $\zeta = 2\sigma$, 4σ, 6σ, 8σ respectively.

Table 5. The first sector lists the exponents $p_{\pm}$ for the EZ interacting herding model, and the second sector includes $p_{\pm}$ for its variant with exogenous driving forces.

ζ	2σ	4σ	6σ	8σ
τ_-	1.58	2.51	3.07	3.24
p_-	0.46 (1)	0.58 (2)	0.65 (1)	0.70 (2)
τ_+	2.67	2.13	1.94	1.71
p_+	0.44 (2)	0.52 (1)	0.58 (2)	0.62 (2)
τ_-	1.33	2.08	2.88	3.99
p_-	0.55 (3)	0.68 (4)	0.77 (3)	0.86 (5)
τ_+	2.07	2.39	2.05	1.96
p_+	0.46 (3)	0.57 (3)	0.63 (3)	0.68 (3)

Fitting the curves to equation (4), we obtain the exponents $p_{\pm}(t)$. As shown in the first sector of Table 5, $p_{\pm}(t)$ are ζ-dependent, and the difference of p_- and p_+ is small. Therefore, this model could be compared with the high-frequency data, although its exponents $p_{\pm}(t)$ are larger. Actually, one may define the volatility $|R| = s^{\alpha}$ with $\alpha \neq 1$ to change the values of $p_{\pm}(t)$.

To simulate the dynamic relaxation before and after the extreme volatilities at the daily time scale, we may introduce exogenous driving forces to the interacting herding model. Here we present a simple scheme. At a certain time, we randomly select several pairs of clusters, and combine each pair into a bigger cluster. As shown in Figure 6b and the second sector of Table 5, such a simple scheme does enhance the time-reversal asymmetry in the dynamic relaxation before and after extreme volatilities. To achieve an accurate comparison with the crude oil markets, one needs more sophisticated exogenous driving schemes, e.g., to modify the dynamic rules for the exogenous events.

6 Conclusions

Using concepts and methods from statistical physics, we have investigated the extreme-volatility dynamics in crude oil markets, based on the high-frequency data of fuel oil prices and the daily data of crude oil prices. The dynamic relaxation is characterized by the power law, and the exponents $p_{\pm}$ usually depend on the magnitude of extreme volatilities. The relaxation before and after extreme volatilities is time-reversal symmetric at the high-frequency time scale, i.e., $p_- = p_+$, while it is time-reversal asymmetric at the daily time scale, i.e., $p_- \neq p_+$. This time-reversal asymmetry in the crude oil markets is induced by exogenous events. The dynamic relaxation after exogenous events exhibits the same characteristics as that after endogenous events. Although the extreme-volatility dynamics is rather complicated and may generally depend on the specific markets, an interacting herding model without and with exogenous driving forces could qualitatively describe the extreme-volatility dynamics.

Author contribution statement

X.F.J. and B.Z. conceived the study. X.F.J., B.Z., T.Q. and F.R. designed and performed the research. X.F.J. drafted the manuscript. B.Z. reviewed and approved the manuscript.

This work was supported in part by NNSF of China under Grants Nos. 11505099, 11375149 and 11175079, Zhejiang Provincial Non-Profit Fund for Applied Research under Grant No. 2016C33248, Ningbo Natural Science Foundation under Grant No. 2015A610160, Fok Ying Tong Education Foundation under Grant No. 132013.

References

1. S.H. Kang, S.M. Kang, S.M. Yoon, Energy Economics **31**, 119 (2009)
2. Y. Wei, Y. Wang, D. Huang, Energy Economics **32**, 1477 (2010)
3. S. Mirmirani, H.C. Li, Advances in Econometrics **19**, 203 (2005)
4. W. Xie, L. Yu, S.Y. Xu, S.Y. Wang, in *Computational Science–ICCS 2006* (Springer, 2006), pp. 444–451
5. J.L. Zhang, Y.J. Zhang, L. Zhang, Energy Economics **49**, 649 (2015)
6. Y.D. Wang, L. Liu, X.D. Diao, C.F. Wu, Energy Economics **51**, 599 (2015)
7. H. Naser, Energy Economics **56**, 75 (2016)

8. H.G. Huntington, Energy J. **15**, 1 (1994)
9. W.J. Xie, Z.Q. Jiang, W.X. Zhou, Economic Modelling **36**, 8 (2012)
10. D. Sornette, R. Woodard, W.X. Zhou, Physica A **388**, 1571 (2009)
11. X. Zhang, K.K. Lai, S.Y. Wang, Energy Economics **30**, 905 (2008)
12. L. Yu, K.K. Lai, S.Y. Wang, K.J. He, Lect. Notes Comput. Sci. **4489**, 925 (2007)
13. X. Gabaix, P. Gopikrishnan, V. Plerou, H.E. Stanley, Nature **423**, 267 (2003)
14. R.N. Mantegna, H.E. Stanley, Nature **376**, 46 (1995)
15. R.N. Mantegna, H.E. Stanley, Nature **383**, 587 (1996)
16. X. F. Jiang, B. Zheng, Europhys. Lett. **97**, 48006 (2012)
17. X.F. Jiang, T.T. Chen, B. Zheng, Sci. Rep. **4**, 5321 (2014)
18. B. Zheng, X.F. Jiang, P.Y. Ni, Chinese Phys. B **23**, 078903 (2014)
19. L. Kristoufek, Energy Economics **45**, 1 (2014)
20. F. Lillo, R.N. Mantegna, Phys. Rev. E **68**, 016119 (2003)
21. F. Omori, J. Coll. Sci., Imp. Univ. Tokyo **7**, 111 (1894)
22. F. Selcuk, Physica **A333**, 306 (2004)
23. G.H. Mu, W.X. Zhou, W. Chen, J. Kertész, New J. Phys. **7**, 075037 (2010)
24. A.M. Petersen, F. Wang, S. Havlin, H.E. Stanley, Phys. Rev. E **81**, 066121 (2010)
25. L. Tan, B. Zheng, J.J. Chen, X.F. Jiang, PLoS One **10**, e0118399 (2015)
26. X.F. Jiang, T.T. Chen, B. Zheng, Physica A **392**, 5369 (2013)
27. B. Zheng, Int. J. Mod. Phys. B **12**, 1419 (1998)
28. B. Zheng, M. Schulz, S. Trimper, Phys. Rev. Lett. **82**, 1891 (1999)
29. Y. Liu, P. Gopikrishnan, P. Cizeau, M. Meyer, C.K. Peng, H.E. Stanley, Phys. Rev. E **60**, 1390 (1999)
30. A. Admati, P. Pfleiderer, Rev. Financ. Stud. **1**, 3 (1988)
31. T. Qiu, B. Zheng, F. Ren, S. Trimper, Physica A **378**, 387 (2007)
32. D. Sornette, Phys. Rep. **378**, 1 (2003)
33. D. Sornette, Y. Malevergne, J.F. Muzy, *Application of Econophysics* (Springer, Tokyo, 2004)
34. J.J. Chen, B. Zheng, L. Tan, PLoS One **8**, e79531 (2013)
35. Z.-Q. Jiang et al., J. Economic Behavior and Organization **74**, 149 (2010)
36. Y. Hamao, R.W. Masulis, V. Ng,, Review of Financial studies **3**, 281 (1990)
37. V. M. Eguiluz, M.G. Zimmermann, Phys. Rev. Lett. **85**, 5659 (2000)
38. B. Zheng, F. Ren, S. Trimper, D.F. Zheng, Physica A **343**, 653 (2004)
39. B. Zheng, T. Qiu, F. Ren, Phys. Rev. E **69**, 046115 (2004)